

Letter to the Editor

Reduced immunoglobulin gene diversity in patients with Cornelia de Lange syndrome

To the Editor:

B cells rely on a broad receptor repertoire to provide protection against a wide range of pathogens. This is in part achieved through V(D)J recombination, which, by assembling various combinations of variable (V), diversity (D), and joining (J) genes, creates different IgV regions.¹ The recombination processes are initiated by recombination-activating gene (RAG) 1/RAG2

© 2017 The Authors. Published by Elsevier Inc. on behalf of the American Academy of Allergy, Asthma & Immunology. This is an open access article under the CC BY-NC-ND license (<http://creativecommons.org/licenses/by-nc-nd/4.0/>).

enzymes and requires a functional nonhomologous end-joining (NHEJ) machinery. B cells can further diversify their IgV regions through somatic hypermutation (SHM) to improve affinity between the antibody and antigen and switch the isotype of antibody produced by class-switch recombination (CSR). Both processes are initiated by activation-induced cytidine deaminase (AID) and rely on transcription and a number of DNA repair mechanisms.

Cornelia de Lange syndrome (CdLS) is a rare multisystem developmental disorder characterized by typical facial features, intellectual disability, and multiple congenital anomalies.² Most patients with CdLS have deleterious mutations in the gene encoding the cohesin loader Nipped-B-like (NIPBL), but mutations in the other cohesin-related genes *SMC1A*, *SMC3*, *PDS5B*, *RAD21*, or *HDAC8* have also been identified in selected

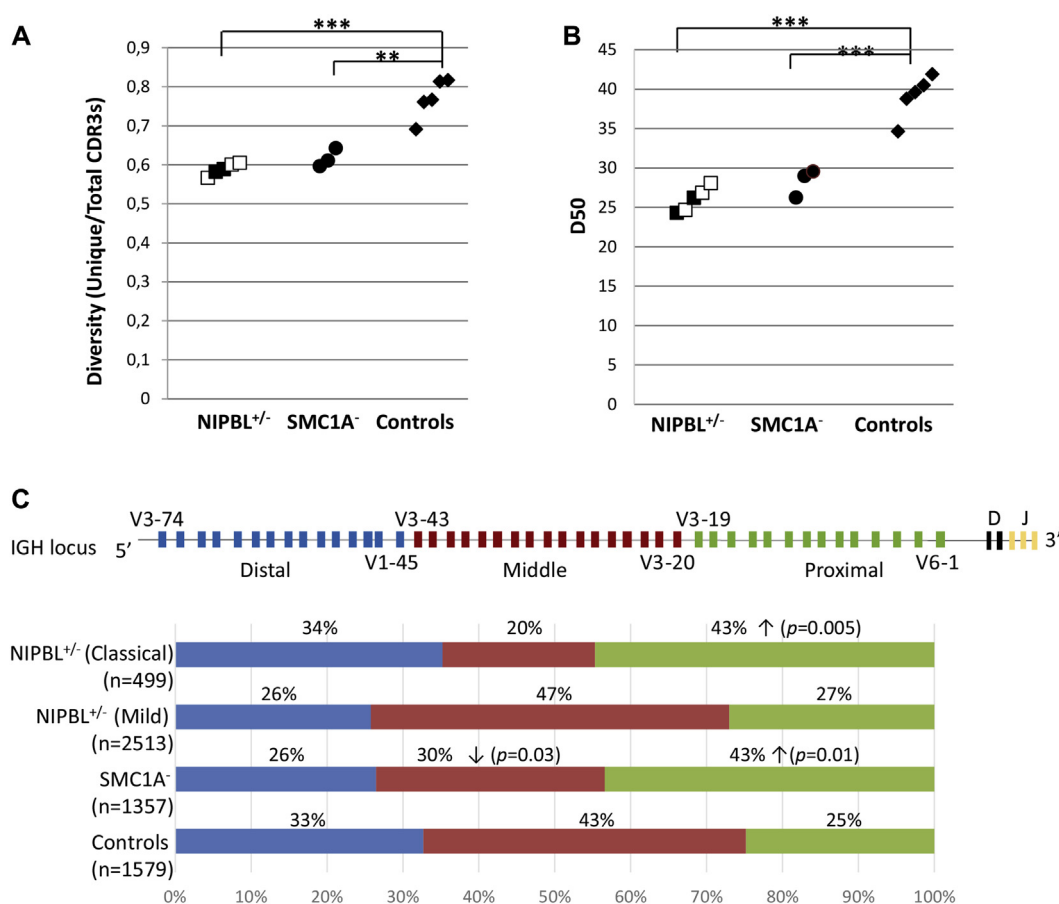


FIG 1. Reduced IGH diversities and increased use of proximal *IGHV* genes in patients with CdLS. **A** and **B**, Diversities (unique/total CDR3s; Fig 1, A) and the proportion of unique B-cell clones (Fig 1, B) that account for D50. Significant differences compared with control values: ** $P < .01$ and *** $P < .001$, Student *t* test. Each dot represents 1 subject. Black or white squares indicate patients with *NIPBL* mutations with the classical or mild form of disease, respectively. **C**, Average frequencies of proximal, middle, and distal *V* genes (in relation to *D* and *J* genes) in patients with CdLS. Schematic picture (not to scale) of the *IGH* locus is shown at top. Proximal, middle, or distal *V* gene groups each encompass approximately 250 kb of the *IGHV* locus and contain 15, 20, and 19 functional *V* genes, respectively. The number of sequences used in the analysis is indicated below each group. The proportion of proximal, middle, or distal *V* genes for each subject was regarded as 1 data point, and the patient and control groups were then compared by using the Student *t* test. Significant differences compared with control values are indicated by arrows. ↑ and ↓, Increased or decreased compared with control values, respectively.

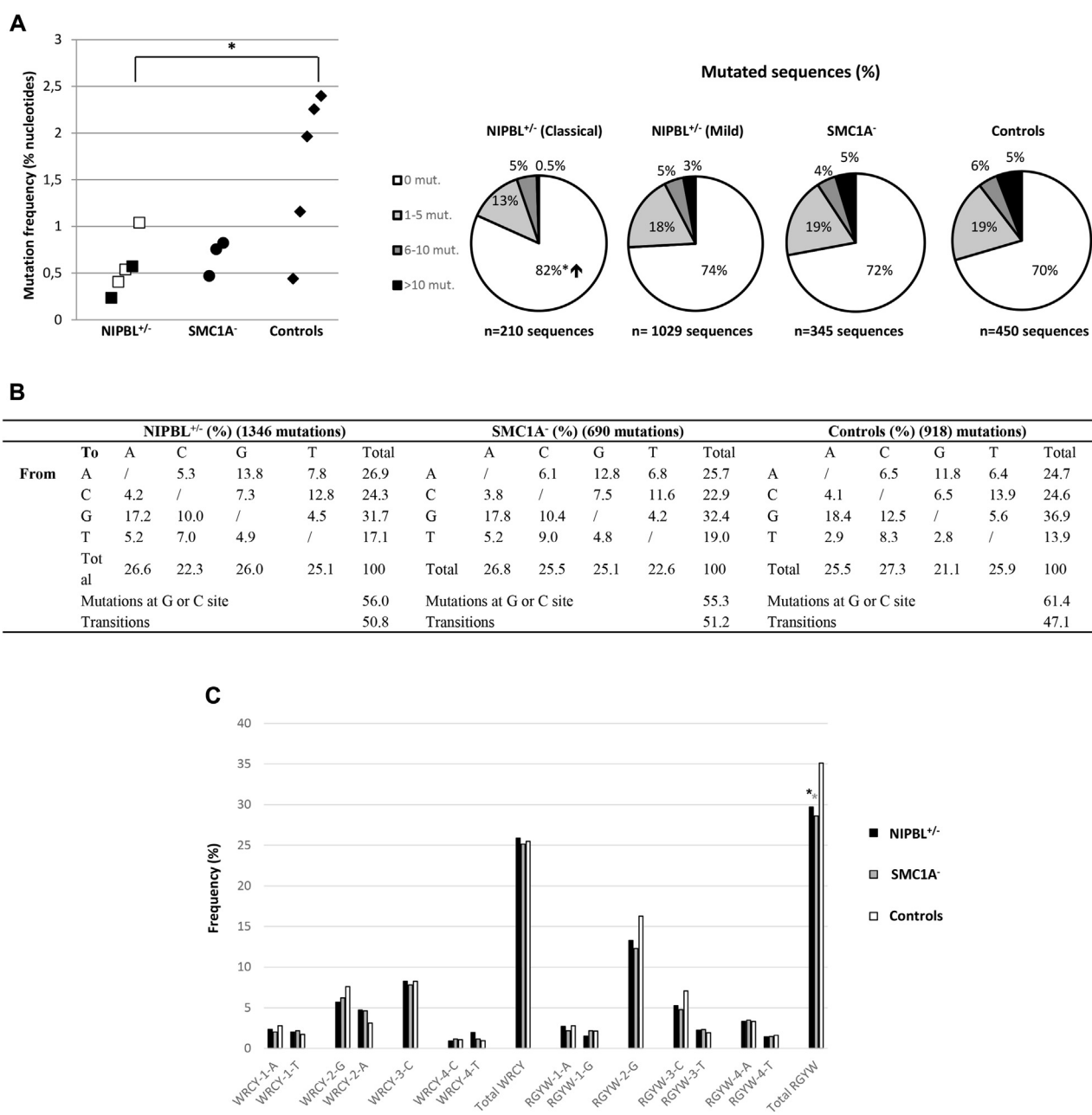


FIG 2. Mutation frequency and substitution pattern in *IGHV* regions from *NIPBL*^{+/-} and *SMC1A*⁻ B cells. **A**, Mutation frequencies are shown at left. Each dot represents 1 subject. Black or white squares indicate *NIPBL*^{+/-} patients with a classical or mild form of disease, respectively. Percentages of sequences with 0, 1 to 5, 6 to 10, or more than 10 mutations in the *IGHV* regions from control, *NIPBL*^{+/-}, or *SMC1A*⁻ cells are depicted in pie charts at right. *IGHV1-18*, *IGHV1-69*, *IGHV3-23*, *IGHV3-30*, *IGHV3-33*, and *IGHV4-34* sequences were included in the analysis. Significant differences compared with control values: *P < .05, Student *t* test. **B**, Frequencies of substitutions in the *IGHV* genes (χ^2 test, Bonferroni corrected). **C**, Frequency of mutations within W(A/T)R(G/A)CY(C/T)/RGYW motifs in the *IGHV* genes analyzed in Fig 2, A. Asterisks indicate significant differences between *NIPBL*^{+/-} (black asterisks) and *SMC1A*⁻ (gray asterisks) compared with control cells. *P < .05, χ^2 test, Bonferroni corrected.

patients. Cohesin has been implicated in regulation of sister chromatid cohesion, transcription, long-range gene interactions, and DNA repair.³

Aberrant CSR patterns have been observed in B cells from patients with *NIPBL* mutations.⁴ Here we further investigated whether V(D)J recombination or SHM is affected in patients with CdLS. In chromosome-integrated V(D)J reporter assays,

a reduced substrate recombination efficiency was observed in *NIPBL* knockdown human fibroblast or murine pro-B cells (see Fig E1 and the Methods section in this article's Online Repository at www.jacionline.org).

We next analyzed the *IGH* repertoire in 5 patients with *NIPBL* mutations and 3 patients with *SMC1A* mutations with CdLS (see Table E1 in this article's Online Repository at

www.jacionline.org). The overall diversity of the *IGHV* repertoire, which is estimated by either the proportion of sequences with a unique complementary determining region 3 (CDR3) divided by the total number of sequences or by cumulative 50% of the total CDR3s in the samples (diversity 50 [D50]), which is a measurement of the evenness of the distribution of B-cell clones, was significantly lower in patients with *NIPBL* or *SMC1A* mutations (Fig 1, A and B). Thus the patients with CdLS had a reduced overall diversity of their *IGHV* regions, with an overrepresentation of large B-cell clones.

Furthermore, in patients with *NIPBL* mutations with the classical form of the disease and in patients with *SMC1A* mutations, the frequency of *IGHV* genes located in the most proximal one third of the *IGH* locus (about 250 kb) was increased (Fig 1, C, and see Fig E2 in this article's Online Repository at www.jacionline.org). The observed skewed pattern of *VH* genes in the patients is likely to be a result of B cell–intrinsic changes because only sequences resulting from unproductive rearrangement (successfully rearranged but out of reading frame or containing stop codons) were included in this analysis, and an influence of antigen selection can thus be excluded.

The overall mutation frequency in the unproductive and most commonly mutated *IGHV* genes was also reduced in the patients with CdLS, reaching statistical significance for the group with an *NIPBL* mutation (Fig 2, A). The proportion of unmutated sequences was increased in the patients with *NIPBL* mutations, especially in those with the classical form of the disease (Fig 2, A). However, the pattern of base pair substitution in the V regions was largely normal in the patients (Fig 2, B).

Our data suggest that the cohesion-associated proteins NIPBL and SMC1A are involved in regulation of V(D)J recombination in human B cells, possibly through regulation of locus contraction. Increased use of proximally located *IghV* genes has previously been observed in mice deficient in factors associated with locus contraction, such as Ikaros, Yin Yang 1, and Pax5, and the cohesin interaction partner CCCTC-binding factor has been suggested to regulate locus contraction and V(D)J recombination at the mouse *Igh* locus.⁵⁻⁷

Another possible explanation of how NIPBL/SMC1A could affect V(D)J recombination could be a change in regulation of DNA repair. We have previously observed a correlation between heterozygous *NIPBL* loss-of-function mutations and increased sensitivity to γ -radiation and a shift toward use of microhomology-based end-joining during CSR, suggesting that NIPBL regulates the NHEJ process.⁴ However, the V(D)J coding junctions generated *in vivo* in patients with CdLS showed a normal repair pattern (see Table E2 in this article's Online Repository at www.jacionline.org). Furthermore, expression of a number of key V(D)J recombination factors was largely normal in *NIPBL* knockout cells (see Fig E3, B, in this article's Online Repository at www.jacionline.org). Thus the core NHEJ machinery appears to be retained in patients with CdLS.

We also found a reduced frequency of mutations within the *IGHV* regions in patients with CdLS. NIPBL and SMC1A could both be involved in the SHM process through regulation of transcription or RNA polymerase pausing, which promotes formation of single-stranded DNA and AID targeting. In support of this notion, there was a reduced number of mutations observed in the RGYW motifs (containing the AID hotspot in the bottom strand) in *NIPBL*^{+/−} and *SMC1A*[−] cells, suggesting an impaired mutagenesis of C residues on the bottom strand (Fig 2, C).

We have previously observed the opposite pattern in NBS1-deficient cells.⁸ Thus the targeting of AID and/or linked repair seem to be asymmetric during SHM, and this can be regulated by a number of factors, including the cohesin-associated factors.

CdLS is not traditionally considered an immunodeficiency disorder, but these patients have an increased prevalence of severe infections.⁹ Immunodeficiency, including mild B-cell lymphopenia, reduced switched memory B-cell numbers, and/or reduced serum immunoglobulin levels, has been observed in previous case reports⁹ and in our own patients (see Table E3 in this article's Online Repository at www.jacionline.org). Complete knockout of *NIPBL* is incompatible with survival, and heterozygous nonsense mutation or frameshift deletions in *NIPBL* are usually associated with a more severe clinical phenotype than those with missense mutations and in frame deletions (classical vs mild form), suggesting a dose-dependent role of the cohesin-associated proteins. The *SMC1A* mutations are missense or in-frame deletions and are generally associated with a milder CdLS phenotype. Thus mutations identified in patients with CdLS can be considered hypomorphic and/or result in haploinsufficiency, and a more significant alteration in immunoglobulin gene diversifications and a more severe immunodeficiency would be expected in the event of a complete loss of these cohesin-associated proteins.

In summary, the less diversified *VH* genes caused by reduced efficiency of V(D)J recombination together with inefficient CSR efficiency might contribute to the frequent infections in patients with CdLS.

Andrea Björkman, PhD^{a*}

Likun Du, PhD^{a*}

Mirjam van der Burg, PhD^b

Valerie Cormier-Daire, MD^c

Guntram Borck, PhD^d

Juan Pié, MD^e

Britt-Marie Anderlid, MD^f

Lennart Hammarström, MD, PhD^a

Lena Ström, PhD^g

Jean-Pierre de Villartay, PhD^h

David Kipling, PhDⁱ

Deborah Dunn Walters, PhD^{j,k}

Qiang Pan-Hammarström, MD, PhD^a

From the Departments of ^aLaboratory Medicine and ^aCell and Molecular Biology, Karolinska Institutet, Stockholm, Sweden; ^bthe Department of Immunology, Erasmus MC, Rotterdam, The Netherlands; ^cthe Department of Genetics, INSERM U781, Hospital Necker, Paris, France; ^dthe Institute of Human Genetics, University of Ulm, Ulm, Germany; ^ethe Unit of Clinical Genetics and Functional Genomics, Departments of Pharmacology-Physiology and Pediatrics, School of Medicine, University of Zaragoza, Zaragoza, Spain; ^fthe Department of Clinical Genetics, Karolinska University Hospital, Stockholm, Sweden; ^gUniversité Paris-Descartes, Faculté de Médecine René Descartes, Site Necker, Institut Fédératif de Recherche, Paris, France; ^hthe Division of Cancer and Genetics, School of Medicine, Cardiff University, Cardiff, United Kingdom; ⁱthe Department of Immunobiology, King's College London School of Medicine, London, United Kingdom; and ^jthe Faculty of Health & Medical Sciences, University of Surrey, Guildford, United Kingdom. E-mail: qiang.pan-hammarstrom@ki.se.

*These authors contributed equally to this work.

Supported by the European Research Council (242551-ImmunoSwitch), Swedish Research Council, Swedish Cancer Society, Center for Innovative Medicine at Karolinska Institutet (CIMED), and Swedish Childhood Cancer Foundation.

REFERENCES

- Schatz DG, Ji Y. Recombination centres and the orchestration of V(D)J recombination. *Nat Rev Immunol* 2011;11:251-63.
- Liu J, Baynam G. Cornelia de Lange syndrome. *Adv Exp Med Biol* 2010;685: 111-23.
- Mehta GD, Kumar R, Srivastava S, Ghosh SK. Cohesin: functions beyond sister chromatid cohesion. *FEBS Lett* 2013;587:2299-312.

4. Enervald E, Du L, Visnes T, Bjorkman A, Lindgren E, Wincent J, et al. A regulatory role for the cohesin loader NIPBL in nonhomologous end joining during immunoglobulin class switch recombination. *J Exp Med* 2013;210:2503-13.
5. Degner SC, Verma-Gaur J, Wong TP, Bossen C, Iverson GM, Torkamani A, et al. CCCTC-binding factor (CTCF) and cohesin influence the genomic architecture of the IgH locus and antisense transcription in pro-B cells. *Proc Natl Acad Sci U S A* 2011;108:9566-71.
6. Degner SC, Wong TP, Jankevicius G, Feeney AJ. Cutting edge: developmental stage-specific recruitment of cohesin to CTCF sites throughout immunoglobulin loci during B lymphocyte development. *J Immunol* 2009;182:44-8.
7. Guo C, Yoon HS, Franklin A, Jain S, Ebert A, Cheng HL, et al. CTCF-binding elements mediate control of V(D)J recombination. *Nature* 2011;477:424-30.
8. Du L, Dunn-Walters DK, Chrzanowska KH, Stankovic T, Kotnis A, Li X, et al. A regulatory role for NBS1 in strand-specific mutagenesis during somatic hypermutation. *PLoS One* 2008;3:e2482.
9. Jyonouchi S, Orange J, Sullivan KE, Krantz I, Deardorff M. Immunologic features of Cornelia de Lange syndrome. *Pediatrics* 2013;132:e484-9.

<http://dx.doi.org/10.1016/j.jaci.2017.06.043>

METHODS**Patients**

Eight patients with CdLS were included in the study (Table E1). Five had heterozygous mutations in the *NIPBL* gene, 2 of whom (P3 and P6) had a more severe classical form of CdLS, whereas 3 (P8, P10, and P11) had a milder form of disease. In addition, 3 male patients had mutations within the *SMC1A* gene, which was located on the X-chromosome (SMC1A-1, SMC1A-2, and SMC1A-4). The clinical features of 7 of the 8 patients have been described previously.^{E1-E4} Seven unaffected control subjects were also included in the study (Table E1). DNA was isolated from peripheral blood by using standard methods. The study was approved by the institutional review board at the Karolinska Institutet.

V(D)J recombination substrate assays for assessment of recombination efficiency

The retroviral vector pMX-RSS-green fluorescent protein (GFP)/internal ribosomal entry site (IRES)-hCD4 (MX-RSS-INV), which contains an antisense-orientated RSS-flanked enhanced GFP reporter and an IRES-linked human CD4 cassette,^{E5} was transduced into HEK293FT cells together with 3 viral packaging vectors (pGag-Pol, pRev, and pVSV-G) by using Lipofectamine 2000 (Thermo Fisher Scientific, Waltham, Mass). Forty-eight hours later, the medium containing virus was collected and used to infect the human fibroblast cell line from an unaffected control subject. Seventy-two hours later, the transduced cells were sorted by means of flow cytometry with human CD4 antibody (BioLegend, San Diego, Calif). The CD4⁺ cells were expanded in culture for 4 days and then seeded into 6-well plates (10⁵ cells per well) and treated with either NIPBL or control small interfering RNA (siRNA; GE Dharmacon, Lafayette, Colo)^{E4} for 48 hours. The cells were subsequently transfected with 0.9 µg of RAG1 and 0.75 µg of RAG2 plasmids by using TurboFect (Fermentas, Waltham, Mass). Forty-eight hours after transfection, cells were collected, and recombination activity was assessed as percentages of GFP⁺ cells by using flow cytometry. This chromosome-integrated reporter assay allows assessment of V(D)J recombination and infection efficiency through measurement of expression of GFP or CD4, respectively. Gene knockdown efficiency was monitored by using real-time PCR (see Fig E1, B), as described previously.^{E4}

A murine B-abl pro-B-cell line (with a *Bcl2* transgene) carrying the chromosome-integrated MX-RSS-INV substrate was previously described.^{E6} Cells were treated with either *Nipbl* or control smart pool mouse siRNA (GE Dharmacon) by using a Nucleofector Kit (Lonza, Basel, Switzerland) for 48 hours and then treated with 0.3 µmol/L abl kinase inhibitor (PD-180970; Sigma-Aldrich, St Louis, Mo), which leads to G1 cell-cycle arrest and an induction/stabilization of expression of RAG1/RAG2.^{E7} Recombination activity was subsequently assessed as a percentage of GFP⁺ cells by using flow cytometry. Gene knockdown efficiency was monitored by means of real-time PCR (Fig E1, C).

Amplification and high-throughput sequencing of *IGHV* regions from patients with CdLS

Immunoglobulin genes were amplified by using a seminested PCR, as previously described,^{E8} with the exception that 100 ng of genomic DNA and 250 nmol/L of each downstream *IGHJ* primer were used in the PCR reaction. Sequencing was performed on the Roche 454 GS FLX Titanium Sequencer (Agowa GmbH, Berlin, Germany). V-QUEST,^{E9,E10} allowing detection of indels, was used to determine the amino acid sequence of CDR3, as well as the V, D, and J genes used. Sequences not spanning the V(D)J junction were removed, and the remaining sequences were used in subsequent analyses. Therefore any large deletions that resulted in missing an entire CDR3 would not be recorded. The D50 value was calculated by dividing X by Y and multiplying by 100, where X is the number of unique CDR3s that account for the cumulative 50 percent of the total sequences and Y is

number of unique CDR3s. A sample with an equal distribution of all clones would have a D50 of 50, whereas a number less than 50 indicates the presence of uneven larger clones.^{E11} Chimeric sequences, which are artifacts created during the PCR reaction that contains more than 1 *IGHV* region, were detected by means of visual inspection. If the sequence matched more than 1 *IGHV* gene at either end, the sequence was omitted from *IGHV* gene use analysis. For SHM analysis, chimeric sequences were also omitted, unless the sequence was chimeric at the first half of the *IGHV* region sequence, when the remaining part was still included in the analysis. Only unique and unproductive sequences (*VH* and *JH* genes are not in the same reading frame or containing premature stop codons) were included for the *VH* gene use and SHM analyses to avoid any antigen selection bias from the expressed repertoire. The error rate of 454 sequencing was previously determined to be less than 1 error per 1300 bp when indels were excluded.^{E8}

Real-time PCR

One microgram of total RNA was used to synthesize cDNA, according to the manufacturer's protocol (cDNA synthesis kit; GE Healthcare, Piscataway, NJ). Expression of human *XRCC6*, *LIG4*, *DCLRE1C*, *PRKDC*, or *NIPBL* in the fibroblast cell line treated with control or *NIPBL* siRNA was determined by means of quantitative real-time PCR assays with a similar setting, as described previously.^{E4} Primer sequences are available on request. Briefly, real-time PCR amplification was performed with the Kapa SYBR Fast qPCR Master Mix Kit (Kapa Biosystems, Wilmington, Mass). *ACTB* was used as a housekeeping gene for calculation of relative expression levels. Expression of *Nipbl* in the murine B-abl pro-B-cell line treated with control or *Nipbl* siRNA was determined by using a similar strategy, with mouse glyceraldehyde-3-phosphate dehydrogenase (*Gapdh*) as the housekeeping gene.

REFERENCES

- E1. Pie J, Gil-Rodriguez MC, Ciero M, Lopez-Vinas E, Ribate MP, Arnedo M, et al. Mutations and variants in the cohesion factor genes NIPBL, SMC1A, and SMC3 in a cohort of 30 unrelated patients with Cornelia de Lange syndrome. *Am J Med Genet A* 2010;152A:924-9.
- E2. Schoumans J, Wincent J, Barbaro M, Djureinovic T, Maguire P, Forsberg L, et al. Comprehensive mutational analysis of a cohort of Swedish Cornelia de Lange syndrome patients. *Eur J Hum Genet* 2007;15:143-9.
- E3. Borck G, Zarhrate M, Bonnefont JP, Munnoch A, Cormier-Daire V, Colleaux L. Incidence and clinical features of X-linked Cornelia de Lange syndrome due to SMC1L1 mutations. *Hum Mutat* 2007;28:205-6.
- E4. Enervald E, Du L, Visnes T, Bjorkman A, Lindgren E, Wincent J, et al. A regulatory role for the cohesin loader NIPBL in nonhomologous end joining during immunoglobulin class switch recombination. *J Exp Med* 2013;210:2503-13.
- E5. Liang HE, Hsu LY, Cado D, Cowell LG, Kelsoe G, Schlissel MS. The "dispensable" portion of RAG2 is necessary for efficient V-to-DJ rearrangement during B and T cell development. *Immunity* 2002;17:639-51.
- E6. Lescalle C, Abramowski V, Bedora-Faure M, Murigneux V, Vera G, Roth BD, et al. RAG2 and XLF/Cernunnos interplay reveals a novel role for the RAG complex in DNA repair. *Nat Commun* 2016;7:10529.
- E7. Bredemeyer AL, Sharma G, Huang C, Helmink BA, Walker LM, Khor KC, et al. ATM stabilizes DNA double-strand-break complexes during V(D)J recombination. *Nature* 2006;442:466-70.
- E8. Wu YC, Kipling D, Leong HS, Martin V, Ademokun AA, Dunn-Walters DK. High-throughput immunoglobulin repertoire analysis distinguishes between human IgM memory and switched memory B-cell populations. *Blood* 2010; 116:1070-8.
- E9. Giudicelli V, Brochet X, Lefranc MP. IMGT/V-QUEST: IMGT standardized analysis of the immunoglobulin (IG) and T cell receptor (TR) nucleotide sequences. *Cold Spring Harb Protoc* 2011;2011:695-715.
- E10. Brochet X, Lefranc MP, Giudicelli V. IMGT/V-QUEST: the highly customized and integrated system for IG and TR standardized V-J and V-D-J sequence analysis. *Nucleic Acids Res* 2008;36:W503-8.
- E11. Yang Y, Wang C, Yang Q, Kantor AB, Chu H, Ghosn EE, et al. Distinct mechanisms define murine B cell lineage immunoglobulin heavy chain (IgH) repertoires. *Elife* 2015;4:e09083.

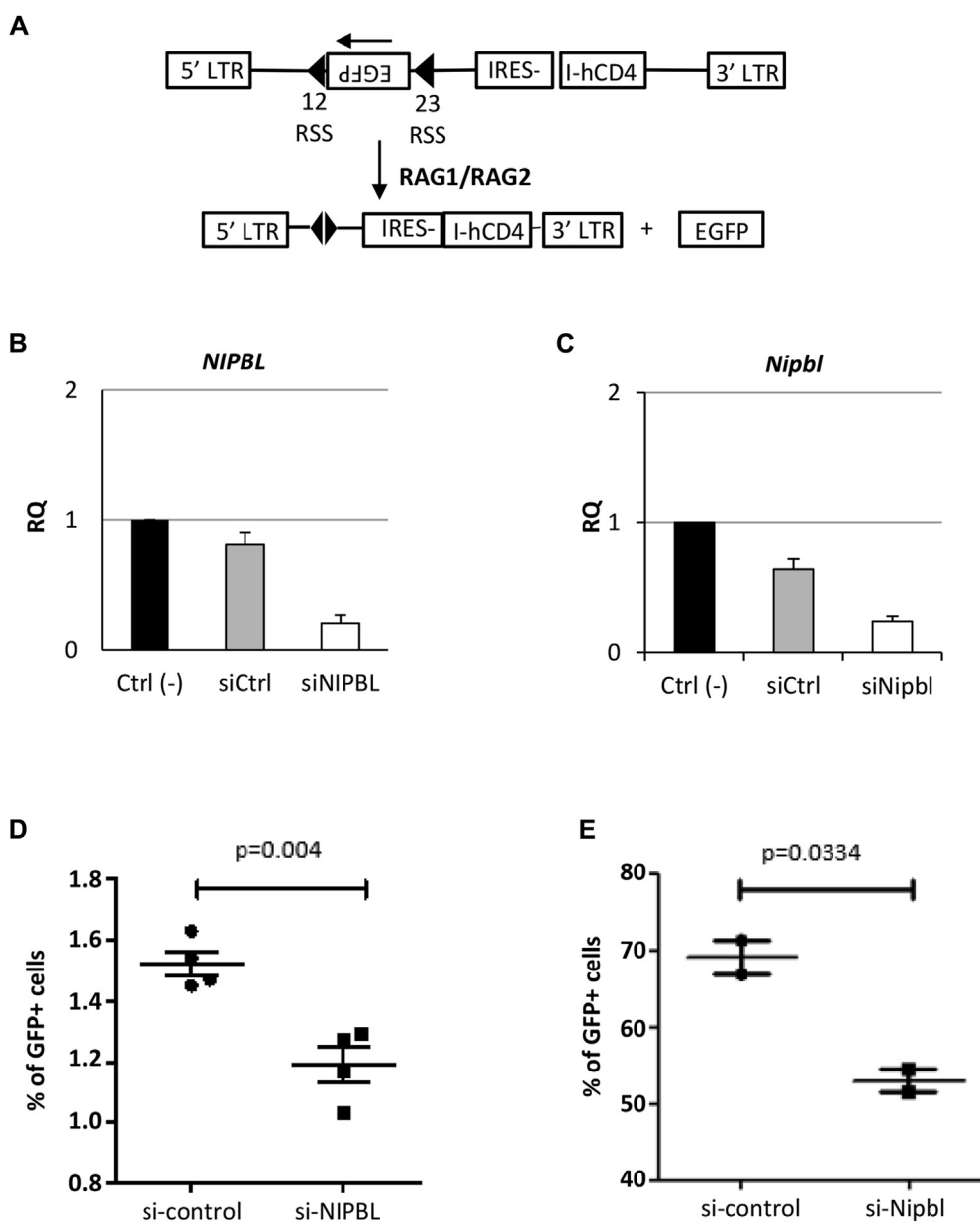


FIG E1. V(D)J recombination substrate assays in a human fibroblast cell line and a murine pro-B-cell line. **A**, Schematic picture of the pMX-RSS-GFP/IRES-hCD4 (MX-RSS-INV) construct. EGFP, Enhanced GFP; LTR, long terminal repeat. **B** and **C**, Expression of *NIPBL* in a human fibroblast line stably transfected with the MX-RSS-INV construct (Fig E1, **B**) and expression of *Nipbl* in a mouse pro-B-cell line stably transfected with the same construct (Fig E1, **C**) were measured by using real-time PCR. Expression of *NIPBL* or *Nipbl* was reduced by 19% or 36% with the scrambled control siRNAs and by 80% or 74% after specific *NIPBL* or *Nipbl* siRNA treatment. RQ, Relative quantification. **D**, Chromosome-integrated V(D)J reporter assay in human fibroblast cells. The V(D)J reporter MX-RSS-INV was retrovirally transduced into a human fibroblast cell line from an unaffected control. CD4⁺ cells were sorted by means of fluorescence-activated cell sorting and expanded and tested (see the Methods section in this article's Online Repository). GFP⁺ cells are indicative of successful recombination. Statistical calculation was performed with the Student *t* test. Results represent 2 independent experiments. **E**, V(D)J reporter assay in a murine B-Abl pro-B-cell line carrying the chromosome integrated MX-RSS-INV substrate. GFP⁺ cells are indicative of successful recombination. Statistical calculation was performed with the Student *t* test. Results represent 2 independent experiments.

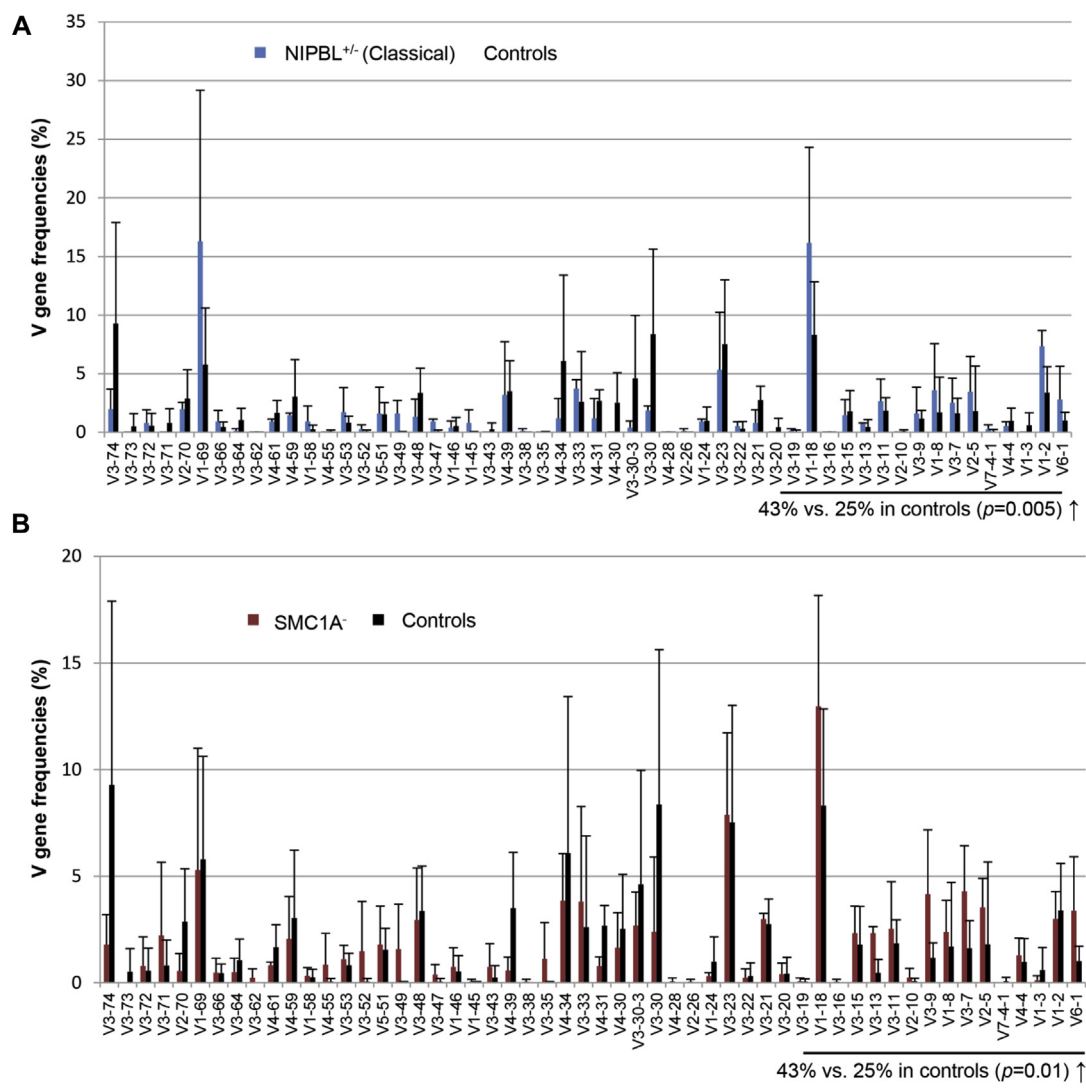


FIG E2. Frequencies of individual *IGHV* genes in unproductive sequences in classical *NIPBL* (A) and *SMC1A*-mutated (B) B cells from patients with CdLS are shown. Statistical calculations were performed by using the Student *t* test, and significant differences compared with control values are indicated by arrows. ↑ and ↓, Increased or decreased compared with control values, respectively.

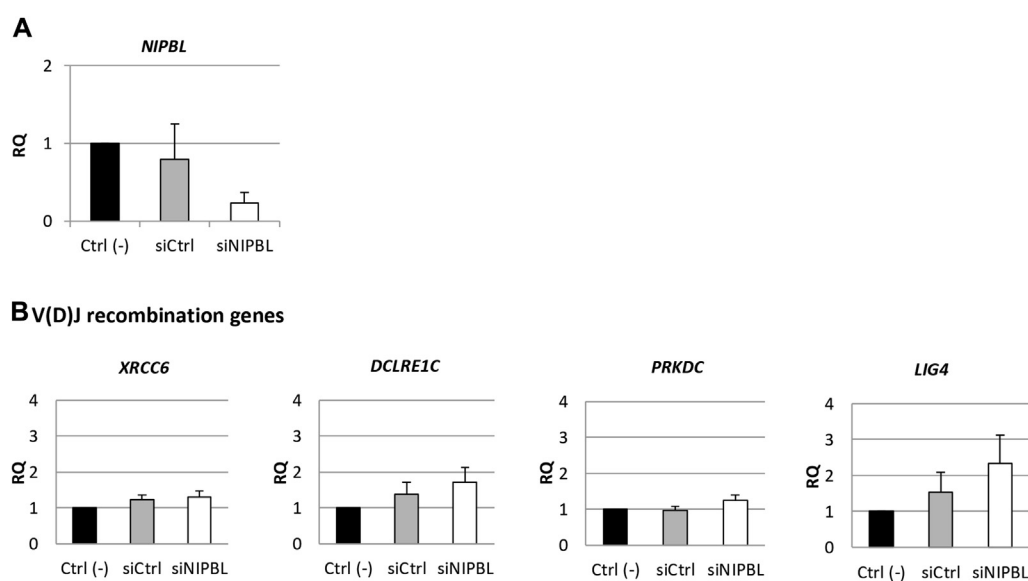


FIG E3. Expression of gene analysis in NIPBL knockdown cells. **A**, Expression of *NIPBL* in a human fibroblast line was measured by using real-time PCR. *NIPBL* expression was reduced by 21% with the scrambled control siRNAs and by 77% after specific *NIPBL* siRNA treatment. **B**, Expression of genes involved in V(D)J recombination in a human fibroblast cell line. Results represent an average of 2 independent experiments. (-), Untreated; *Ctrl*, control; *RQ*, relative quantification.

TABLE E1. Patients included in the study

Patient	Age/sex	Mutation	Diagnosis	Total seq	Productive/unproductive ratio*	Seq with unique CDR3	Diversity†	Unproductive seq with unique CDR3 but not chimeric‡	Reference
P3	17 y/F	NIPBL ^{+/−} , c.6250_6255del, p.V2084-V2085, deletion	Classical CdLS	806	0.69/0.31	475	0.59	125	E2, E4
P6	2 y/M	NIPBL ^{+/−} , c.4593T>A, p.Y1531X, nonsense	Classical CdLS	1,874	0.68/0.32	1,091	0.58	374	E2, E4
P8	4 y/F	NIPBL ^{+/−} , c.4321G>T, p.V1441L, splice site§	Mild CdLS	11,776	0.66/0.34	7,070	0.60	1,938	E1, E4
P10	10 y/M	NIPBL ^{+/−} , c.6242G>C, p.G2081A, missense	Mild CdLS	2,261	0.66/0.34	1,386	0.61	360	E1, E4
P11	14 y/M	NIPBL ^{+/−} , c.8387A>G, p.Y2796C, missense	Mild CdLS	1,191	0.64/0.36	675	0.57	215	This report
SMC1A-1	2 y/M	SMC1A [−] , c.587G>A, p.R196H, missense	CdLS	2,497	0.66/0.34	1,489	0.60	405	E3, E4
SMC1A-2	5 y/M	SMC1A [−] , c.3254A>G, p.Y1085C, missense	CdLS	3,308	0.68/0.32	2,022	0.61	550	E3, E4
SMC1A-4	9 y/M	SMC1A [−] , c.3568A>G, p.K1190E, missense	CdLS	2,163	0.66/0.34	1,390	0.64	402	E4
C19	19 y/M	—	Unaffected	276	0.62/0.38	210	0.76	41	This report
C31	19 y/?	—	Unaffected	316	0.62/0.38	257	0.81	71	This report
C34	13 y/?	—	Unaffected	660	0.65/0.35	506	0.77	113	This report
C54	13 y/?	—	Unaffected	1,840	0.63/0.37	1,272	0.69	321	This report
gCont	2 y, 5 y, 7 y/?	—	Unaffected	3,482	0.53/0.47	2,845	0.82	1,033	This report

F, Female; M, male; Seq, sequence.

*Productive: As a result of V(D)J recombination, the VH, DH, and JH genes are in the correct translational reading frame.

†Diversity was calculated by dividing sequences with unique CDR3s with the total sequences. Sequences not spanning the CDR3 region were omitted from calculation.

‡Only unproductive rearrangement (out of reading frame or containing a stop codon): unique sequences that are not chimeric at both ends were included in V gene analysis.

§This mutation has been shown to yield 2 transcripts, of which one bears an exon 20 deletion and the other is of ordinary size but with a V1441L change.^{E1}

||gCont, Contains a pool of DNA from 3 subjects.

TABLE E2. Characterization* of *in vivo*-generated V(D)J coding junctions†

Study groups	Average CDR3 lengths (bp)	Average no. of palindromic nucleotides (bp)	Average no. of nontemplate nucleotides (bp)
NIPBL ^{+/-}	53.1	0.46	13.5
SMC1A ⁻	53.5	0.50	14.5
Control subjects	53.1	0.48	14.2

*Statistical calculations were performed by using the Student *t* test. No significant differences were found.

†Calculations were based on unique sequences.

TABLE E3. Immunologic data of patients P6, P8, P10, P11, SMC1A-1, and SMC1A-2 with CdLS

	P6 (classical CdLS)	P8 (mild CdLS)	P10 (mild CdLS)	P11 (mild CdLS)	SMC1A-1	SMC1A-2
Age at sampling (y)	14	4	10	14	8	11
Lymphocytes*						
Proportion of lymphocytes	31% (22% to 50%)	NA	35.5% (20% to 45%)	33.4% (20% to 45%)	NA	NA
Total lymphocytes	2100 mm ³ (1000-5500 mm ³)	NA	1700 mm ³ (1500-4500 mm ³)	1700 mm ³ (1500-4500 mm ³)	3400 mm ³	3300 mm ³
T lymphocytes*						
T lymphocytes, CD3 ⁺	84% (52% to 78%)	NA	66% (63% to 84%)	70% (65% to 80%)	NA	NA
T lymphocytes, CD4 ⁺	51% (25% to 48%)	NA	42% (33% to 57%)	33%↓ (40% to 50%)	NA	NA
T lymphocytes, CD8 ⁺	26% (9% to 35%)	NA	20% (14% to 39%)	32% (26% to 30%)	NA	NA
CD4/CD8 ratio	1.96 (0.9-3.4)	NA	2.1 (1.5-2)	1.03↓ (1.5-2)	NA	NA
T lymphocytes, CD4 ⁺	1110 mm ³ (400-2100 mm ³)	NA	715.68 mm ³ (400-1535 mm ³)	551.1 mm ³ (500-800 mm ³)	NA	NA
T lymphocytes, CD8 ⁺	570 mm ³ (200-1200 mm ³)	NA	340.8 mm ³ (139-1015 mm ³)	534.4 mm ³ (250-800 mm ³)	NA	NA
NK cells, CD56 ⁺	5%↓ (6% to 27%)	NA	8% (7% to 21%)	5% (5% to 10%)	NA	NA
B lymphocytes*						
Proportion of B lymphocytes, CD19 ⁺	8% (8% to 24%)	NA	19% (7% to 22%)	19% (10% to 15%)	12%↓ (13% to 27%)	5%↓ (13% to 27%)
Total B lymphocytes, CD19 ⁺	160 mm ³ ↓ (200-600 mm ³)	NA	NA	NA	408 mm ³ (270-860 mm ³)	165 mm ³ ↓ (270-860 mm ³)
CD21 ⁺⁺ CD24 ^{+/} CD19 ⁺	NA	NA	NA	NA	84%	84%
CD21 ⁺ CD24 ⁺⁺ /CD19 ⁺	NA	NA	NA	NA	1.7%	1.2%
CD21 ⁻ CD24 ⁻ /CD19 ⁺	NA	NA	NA	NA	5%	5%
CD27 ^{+/} CD19 ⁺	NA	NA	NA	NA	31% (>10)	16% (>10)
CD27 ^{+/} IgD ⁺ /CD19 ⁺ (marginal zone)	15% (6% to 29%)	NA	NA	NA	21%	8%
IgM ⁺ IgD ⁺ /CD19 ⁺	NA	NA	NA	NA	78%	63%
IgM ⁺ IgD ⁺ /CD27 ^{+/} CD19 ⁺	NA	NA	NA	NA	63%	37%
IgM ⁺ IgD ⁻ /CD27 ^{+/} CD19 ⁺	NA	NA	NA	NA	16%	8%
IgM ⁻ IgD ⁻ /CD27 ^{+/} CD19 ⁺	NA	NA	NA	NA	17% (>10)	46% (>10)
CD21 ⁻ CD38 ⁻ /CD19 ⁺	NA	NA	NA	NA	5%	3.7%
IgD ⁺ CD27 ⁻ (naive)	78% (47% to 84%)	NA	NA	NA	NA	NA

(Continued)

TABLE E3. (Continued)

	P6 (classical CdLS)	P8 (mild CdLS)	P10 (mild CdLS)	P11 (mild CdLS)	SMC1A-1	SMC1A-2
IgD ⁻ CD27 ⁺ (switched memory)	4% ↓ (8% to 29%)	NA	NA	NA	NA	NA
IgM ⁻ CD38 ⁺ (plasmablasts)	1% (0% to 3.2%)	NA	NA	NA	NA	NA
IgM ⁺⁺ CD38 ⁺⁺ (transitional)	<0.5% (<1)	NA	NA	NA	NA	NA
B ⁻ CD21 ⁻ CD38 ⁻ (CD21 low)	1% (<4)	NA	NA	NA	NA	NA
B-cell proliferation†	NA	NA	NA	NA	NA	Normal
Immunoglobulins*						
IgM	1.71 g/L (0.27-2.1 g/L)	0.59 g/L (0.27-2.1 g/L)	56.2 mg/dL ↓ (60-263 mg/dL)	65.4 mg/dL (50-268 mg/dL)	NA	1.47 g/L (0.53-1.62 g/L)
IgG	14.5 g/L (6.1-14.5 g/L)	9.65 g/L (6.1-14.5 g/L)	754 mg/dL ↓ (768-1632 mg/dL)	825 mg/dL (768-1632 mg/dL)	NA	14.97 g/L (6.55-12 g/L)
IgA	2.82 g/L (0.7-3.65 g/L)	0.98 g/L (0.5-2.3 g/L)	63.5 mg/dL ↓ (68-378 mg/dL)	180 mg/dL (68-378 mg/dL)	NA	1.89 g/L (0.5-2.03 g/L)
Immunoglobulin switching‡	NA	NA	NA	NA	NA	Positive but weak
Specific immunoglobulins						
S-Difteri-ak (IgG)	NA	0.2 IE/mL (0.01-3.0 IE/mL)	NA	NA	NA	NA
S-Tetanus-ak (IgG)	NA	0.25 IE/mL (0.09-12.87 IE/mL)	NA	NA	NA	NA
S-Tetanus-ak (IgG ₁)	0.75 mg/L ↓ (4.9-180 mg/L)	2.9 mg/L (0.9-228.5 mg/L)	NA	NA	NA	NA
S-Haemophilus-ak (IgG)	NA	0.14 mg/L ↓ (0.15-29.5 mg/L)	NA	NA	NA	NA
S-Pneumokock-ak (IgG ₂)	NA	11 mg/L (0.8-122.4 mg/L)	NA	NA	NA	NA
S-Pneumokock-ak (IgG)	NA	25 mg/L (9.2-225.9 mg/L)	NA	NA	NA	NA

NA, Not analyzed; NS, nonstimulated; TH3, thymidine incorporation.

*Normal range from the immunologic center where the measurement was taken is indicated in parentheses. Values less than the normal range are indicated in boldface.

†Measured after stimulation with IL-4, CD40L, CD40L plus IL-4, NS-BAFF_TH3, BAFF_TH3, BAFF + μ₊TH3 or CpG + μ₊TH3.

‡Measured after stimulation with CD40L + IL-4 for switching to IgE.